Atmospheric Research 221 (2019) 46–57

Contents lists available at ScienceDirect

Atmospheric Research

journal homepage: www.elsevier.com/locate/atmosres

Stable isotope ($\delta^{18}O$ and δD) dynamics of precipitation in a high altitude Himalayan cold desert and its surroundings in Indus river basin, Ladakh

Suhail A. Lone[a], Ghulam Jeelani[a,*], Rajendrakumar D. Deshpande[b], Abhijit Mukherjee[c,*]

[a] Department of Earth Sciences, University of Kashmir, Srinagar 190006, India
[b] Geoscience Division, Physical Research Laboratory (PRL), Ahmadabad 380009, India
[c] Department of Geology and Geophysics, Indian Institute of Technology, Kharagpur, WB 721302, India

ARTICLE INFO

Keywords:
Indian summer monsoons
Precipitation
Indus basin
Stable isotopes
Himalayas

ABSTRACT

Water resources in the northwestern Himalayas are influenced by the circulation of two dominant weather systems: westerlies and southwest monsoons. The effect of climate change has significantly influenced the overall behaviour of these precipitation bearing climate systems and therefore, the meteorology of the region. To investigate the source, transportation, admixture of vapor sources and post-precipitation modification of stable water isotopic composition ($\delta^{18}O$ and δD) of precipitation in the high altitude Himalayan cold desert of Ladakh, upper Indus river basin (IRB) an observational network was established. Monthly composite ($n = 110$) and event wise precipitation samples ($n = 32$) were collected during the year 2015–16 for stable water isotopes ($\delta^{18}O$ and δD). The stable water isotopic values of the precipitation samples were lower at higher altitude and in January. The monthly $\delta^{18}O$ (and δD) of precipitation showed a negative correlation with altitude ($R^2 = 0.93$, $p = .001$) and temperature ($R^2 = 0.71$ $p = .007$). However, it was perceived that the stable water isotopic value of precipitation abruptly drops at all the precipitation sites in August, without considerable variation in the ambient temperature and precipitation amount signifying the alteration in moisture source. The NCEP/NCAR reanalysis and back trajectory modeling also corroborates and suggests the modification in the moisture source and reversal of wind pattern during this period. The less d-excess and lower slope (7.4) of local meteoric waterline than the global, regional and local meteoric water lines of western Himalayan, central Himalayas and Kashmir Himalayas indicate the secondary evaporation of falling raindrops below the cloud base. Lagrangian moisture diagnostic was used to recognize the sources, which endorsed the quantitative distinction of different evaporative moisture sources.

1. Introduction

The stable water isotopic values of precipitation have been broadly used for hydrological and climatological studies, due to their properties linked with conditions associated to condensation and evaporation of atmospheric moisture (Dansgaard, 1964; Rozanski et al., 1993; Uemura et al., 2012a, 2012b; Wang et al., 2016; Li et al., 2016; Chen et al., 2017). During the last 4 decades, stable water isotopic signatures of precipitation have been used for pursuing atmospheric water vapor cycling processes at different scales, such as long transportation (Dansgaard, 1964; Wang et al., 2017) land-atmosphere moisture exchange (Guan et al., 2013; Bailey et al., 2015; Wang et al., 2016), and cloud-related processes (Crawford et al., 2017). All these studies need a good sympathetic of factors influencing and modifying the stable water isotopic composition of recent precipitation. At high latitudinal area of the globe, the most well-known relationship of stable water isotopes and climate is the linear dependence of precipitation $\delta^{18}O$ on temperature (the temperature effect), while as, in hot and humid regions, an opposite relationship between $\delta^{18}O$ and precipitation amount has been perceived on the temporal time scale mostly in arid climatic regions (Wang et al., 2016, 2017). Moreover, the stable isotopic values are also sensitive to variations in the source of moisture and to the assimilated antiquities of condensation as well as mixing of air mass with the continental moisture source during its transportation (Guan et al., 2013; Bailey et al., 2015; Wang et al., 2016; Jeelani et al., 2017a; Jeelani et al., 2018). In Asia monsoon dominant region, particularly Southeast Asia the precipitation amount effect has been raised to elucidate stable water isotopic variation at the monthly time scale (Dansgaard, 1964; Araguas-Araguas et al., 1998; Breitenbach et al., 2010; Jeelani et al., 2018). However, there are omissions to this reverse

* Corresponding authors.
E-mail addresses: geojeelani@gmail.com (G. Jeelani), amukh2@gmail.com (A. Mukherjee).

https://doi.org/10.1016/j.atmosres.2019.01.025
Received 17 October 2018; Received in revised form 21 January 2019; Accepted 27 January 2019
Available online 28 January 2019
0169-8095/ © 2019 Elsevier B.V. All rights reserved.

relationship (Kurita et al., 2009; Rozanski et al., 1993; Tang et al., 2015). Recent studies advised that stable water isotopes in Southeast Asia are clearly associated to regional climatic processes rather than to local precipitation amount effect (Rozanski et al., 1993; Kurita et al., 2009; Yang et al., 2012). Atmospheric convection and a vapor source of precipitation possibly play a substantial role in the variability of stable water isotopic composition (Aizen et al., 1996; Kang et al., 2002; Aizen et al., 2009; Lyon et al., 2009; Wen et al., 2012; Yao et al., 2013; Tang et al., 2015; Wang et al., 2016; Jeelani et al., 2018). These studies have enhanced the understanding of precipitation stable water isotope systematics of modern precipitation in Himalaya and Southeast Asia. However, the related processes remain a subject of discussion predominantly in arid and semi-arid climatic regions. Uncertainties still occur about climate and stable water isotope relationships, as well as the degree to which climatic variables affect stable water isotopes both at local and regional scale. We aim to explore the source, transportation, admixture of vapor sources and post-precipitation modification of stable water isotopic composition ($\delta^{18}O$ and δD) of precipitation in the high altitude Himalayan cold desert Ladakh, upper (IRB).

2. Study site

The transboundary Indus river basin, disseminated between Pakistan (47%), India (39%), China (8%) and Afghanistan (6%), covering an area of 1.12 million km^2. The study area is a part of the upper Indus basin in India, which is also known as Trans-Himalayas. The area lies between the geographical coordinates of latitudes 32°30′ and 35°00′ N and longitudes 75°50′ to 79°10′ E), covers an area of 59,146 km^2, is surrounded by the higher Himalayan range on east and Karakoram Range towards the north (Fig. 1). The Ladakh, upper Indus basin has a rough topography conquered by barren mountains. Most of the study area lies above 3000 (m, amsl) with little or no vegetation. Ladakh region has 447 glaciers covering an area of 1936 km^2. The area experiences a cold-arid climate with a mean annual temperature of 5.2 °C and precipitation of about 115 mm (Lone et al., 2017), recorded at Indian Meteorological station (IMD), Leh (34°08′09″N and 77°32′47″E).

The precipitation in the northwestern Himalayas is controlled by westerly circulation and southwest monsoons throughout the year

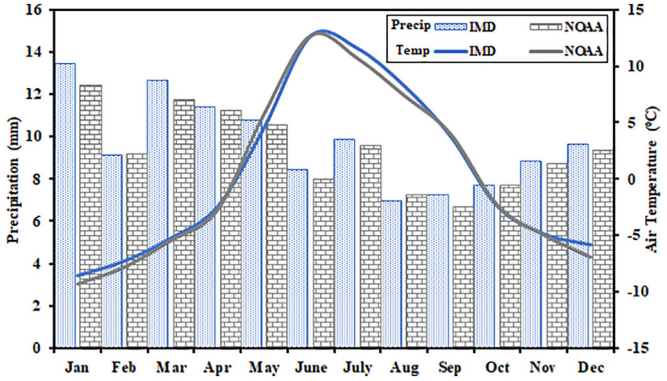

Fig. 2. Average monthly precipitation and temperature from 1980 to 2017 (source IMD [Leh weather station] and NOAA [National oceanic and atmospheric administration]).

(Gadgil, 2003; Tian et al., 2008; Jeelani and Deshpande, 2017). About 86% of mean annual precipitation is recorded from January to May, with the maximum precipitation (13.4 mm) received in the month of January and minimum (6.9 mm) in the month of August (Fig. 2). The maximum daily temperature is perceived in July (14 °C) and the minimum daily temperature is perceived in January (-8 °C).

3. Impact of changing climate on temperature and precipitation

Long-term air temperature and precipitation statistics available suggests an overall rise in temperature and decline in precipitation amount across the Ladakh, upper Indus river basin. Data from IMD (1980–2017) and NOAA (1901–2017) was used as the primary weather data source in this study. Due to unavailability of IMD data from 1901 to 1980 and lack of observed data in other parts of Ladakh, upper IRB. The satellite data from National Oceanic Atmospheric Administration (NOAA) was used. The NOAA data from 1980 to 2017 was first equated with the available IMD data for the similar time period to check its accuracy and it was found that NOAA data closely matches within < 10% with IMD data (Fig. 3).

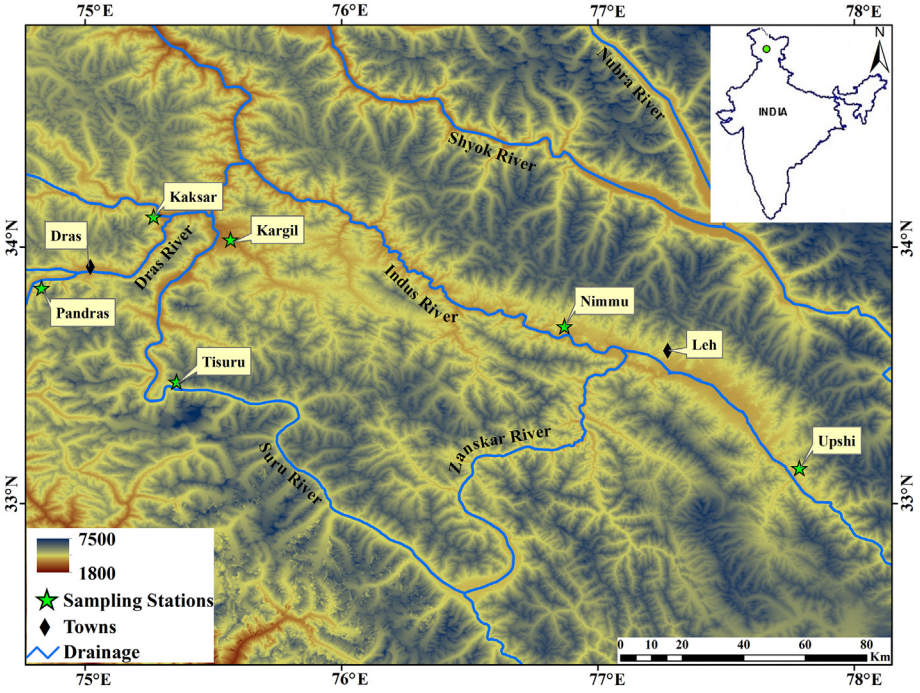

Fig. 1. Upper Indus River Basin, Ladakh (Note: Kargil precipitation station and Kargil town is designated with same symbol).

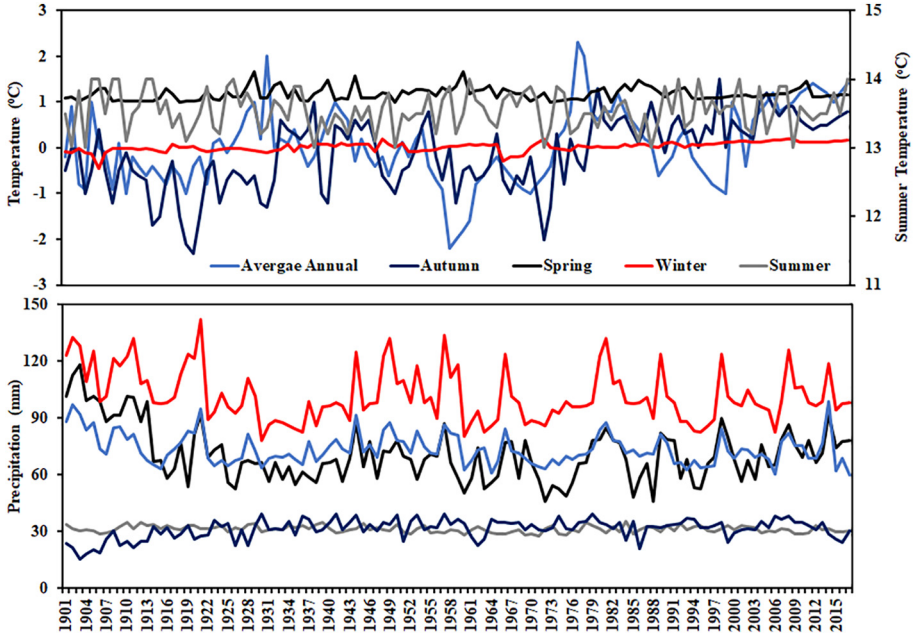

Fig. 3. Seasonal averages of temperature and precipitation; winter (December to February), spring (March to May), summer (June to August), and autumn (September to November) from 1901 to 2017.

Both the data sets (IMD and NOAA) demonstrate an increase of about 0.162 °C (0.0013 °C yr^{-1}) during the 1901–2017 period (Fig. 3). An increase in temperature by 0.02 °C yr^{-1} from 1901 to 1930 followed by an insignificant increase (0.0002 °C yr^{-1}) from 1931 to 1973. A warming trend of about 0.02 °C yr^{-1} was observed from 1974 to 1990 followed by the highest increasing trend (0.09 °C yr^{-1}) from 1991 to 2017. An annual precipitation slightly diminished by about 0.032 mm yr^{-1}. However, an increasing trend in precipitation by about 0.8 mm yr^{-1} was observed from 1910 to 1930 followed by a retreating trend from 1931 to 1944 by about 2.2 mm yr^{-1}. A decreasing trend of 1.9 mm yr^{-1} was observed from 1950 to 2017 (Fig. 3).

The mean periodic temperatures (Fig. 3) show little warming in summer (0.006 °C yr^{-1}) and higher warming in winter (0.08 °C yr^{-1}). Temporally precipitation amount increase in spring (0.21 mm yr^{-1}), summer (0.11 mm yr^{-1}), and autumn (0.09 mm yr^{-1}), while winter precipitation showed a declining trend (0.18 mm yr^{-1}). The similar conclusions are drawn by other studies on changing climate in the northwestern Himalayas (Bhutiyani et al., 2007; Jeelani et al., 2012). The similar positive warming trend is reported in Kosi Basin, Central Himalayas, (Sharma et al., 2000; Shrestha et al., 2019), western Himalayas (Shekhar et al., 2010), Himalayas (Rao et al., 2016) and Bangladesh (Bari et al., 2016).

The results are agreeing with the global warming trends and the studies in other mountainous areas of the globe. Austrian Alps and Bavarian Alps (Auer and Böhm, 1994; Diaz and Bradley, 1997), Swiss Alps (Beniston et al., 1994), French and European Alps (Jamelli et al., 2004; Kohler et al., 2014), Rocky Mountains in Colorado, USA (Ferreira et al., 2018) southern Andes in Argentina, Carpathian region (Kohler et al., 2014) and Chile (Villaba et al., 2003; Vuille et al., 2003) have also presented a rising trend in air temperature in past (Table 1).

4. Sampling

Total (n = 142) precipitation samples were collected at six stations viz.; Pandras (latitude: 34°24′41″N, longitude: 75°37′59″E, elevation: 2875 m, amsl), Kaksar (latitude: 34°31′10″N, longitude: 75°58′22″E, elevation: 2952 m, amsl), Kargil (latitude: 34°33′17″N, longitude: 76°08′03″E, elevation: 3046 m, amsl) Tisuru (latitude: 34°04′17″N, longitude: 75°58′38″E, elevation: 3425 m, amsl), Nimmu (latitude: 34°11′43″N, longitude: 77°20′07″E, elevation: 3142 m, amsl) and Upshi (latitude: 33°50′07″N, longitude: 77°48′54″E, elevation: 3445 m, amsl) and some random samples were also collected at different altitudes across the Ladakh, upper IRB (Fig. 1). The sampling stations were classified depending upon the feasibility in sample collection and geographic extent. Precipitation samples (n = 110) were collected at a monthly basis (n = 32) samples were collected on event basis during 2015–2016. Precipitation samples were collected using a typical rain collector (Gröning et al., 2012) with a long narrow tube attached to the 5-l plastic container, fitted with a funnel, to reduce the evaporative loss of stored rainwater (Gröning et al., 2012; Jeelani et al., 2017a, 2017b, 2017c). Two collectors were installed at each site one for monthly samples and the other for event samples. Each collector was emptied after the sample was collected and dried before its reuse. The event wise samples were collected immediately after the rain stopped. Fresh snow samples in winter were collected as a core using a PVC pipe and transferred in one-litre bottles, covered and permitted to melt at room temperature. Rainwater and the meltwater were transferred to 10 ml polyethylene (PP) bottles.

5. Analysis

The samples were sent to (PRL) Physical Research Laboratory, Geosciences Division Ahmedabad (India), for stable water isotopic analysis. The stable water isotopic ratios of oxygen and hydrogen were measured in an isotope ratio mass spectrometer (Delta V plus, Thermo Scientific) following the standard gas equilibration method (Epstein and Mayeda, 1953; Maurya et al., 2009). For ($\delta^{18}O$ and $\delta^{2}H$) measurements, 300 µl of water was equilibrated with CO_2 for 16 h (or 1 h) and the equilibrated gas was analysed for stable isotopic ratio $^{18}O/^{16}O$ (or $^{2}H/^{1}H$; Maurya et al., 2009). The stable water isotopic results are reported in the standard δ-notation (Coplen, 1996) and demarcated in relation to VSMOW (Vienna Standard Mean Ocean Water). The meteorological parameters (surface air temperature, amount of precipitation) was acquired from IMD (Indian Meteorological Department) and NOAA (National Oceanic and atmospheric administration). To recognize the climate systems resulting in precipitation across the Ladakh the National Centers for Environmental Prediction/National Center for Atmospheric Research (NCEP/NCAR) Reanalysis 1 (Kalnay et al., 1996;

Table 1
Variation of average annual temperature and precipitation at various station in Himalayas and other parts of globe.

Temperature (°C)	Precipitation (mm)	Location	Reference
1.6	–	Northwestern Himalayas	Bhutiyani et al., 2007
2	–	Western Himalayas	Shekhar et al., 2010
0.08	0.28	Kashmir Himalayas	Jeelani et al., 2012
0.90	–	Kosi Basin Himalayas	Sharma et al., 2000
–	−1.27 to 7.4	Central Himalayas	Shrestha et al., 2019
2.5	–	Himalayas	Rao et al., 2016
–	1.28	Bangladesh	Bari et al., 2016
0.4	–	French Alps	Jamelli et al., 2004
0.12 to 2.0	–	European Alps	Kohler et al., 2014
2.4	–	Carpathian region	Kohler et al., 2014

Kistler et al., 2001) at spatial resolutions of 2.5° (latitude) × 2.5° (longitude) was applied (available at http://www.esrl.noaa.gov). The NCEP/NCAR Reanalysis 1 dataset was used to analyse the vector wind and humidity across Ladakh, upper IRB. The monthly data were used in calculating vector wind fields and humidity at 500 hPa. To track the air mass movement, an HYSPLIT (Hybrid Single-Particle Lagrangian Integrated Trajectory) model (Draxler and Hess, 1998; Draxler et al., 2016) version 4 was used for the study. The HYSPLIT model built-up by the Air Resources Laboratory, National Oceanic and Atmospheric Administration, has been broadly used in moisture tracing diagnostics (Bershaw et al., 2012; Salamalikis et al., 2015; Bailey et al., 2015). In the present study, a data set of NCEP/NCAR with a spatial resolution of 2.5° × 2.5° was also employed. The deviation of specific humidity along a trajectory can be checked to estimate the vaporization and precipitation process using a Lagrangian model (Sodemann et al., 2008; Crawford et al., 2017)., the HYSPLIT model was used specifically to calculate the backward trajectories for each precipitation event. All back-trajectories starting at 1000, 1500 and 2000 m AGL (most of the atmospheric processes in Ladakh, IRB takes place within these limits) and were traced back 96 h (average velocity of western disturbances is 13 km/h which takes 3–4 days to reach the study area) before arrival using Global NOAA NCEP/NCAR reanalysis archived data on a latitude-longitude grid (2.5 degrees).

6. Results and discussions

6.1. Isotopic variation in precipitation and the geo-meteorologic controls

During the observation period, the stable water isotopes ($\delta^{18}O$ and δD) in precipitation showed a significant spatial and temporal variation (Table 2). The lower stable isotopic values in precipitation are observed in Leh ($\delta^{18}O$: −12.85‰; δD: −102.8‰), whereas relatively higher isotopic signatures in precipitation are found in Kargil ($\delta^{18}O$: −11.84‰; δD: −86.8‰) and Dras ($\delta^{18}O$: −11.48‰; δD: −77.3‰).

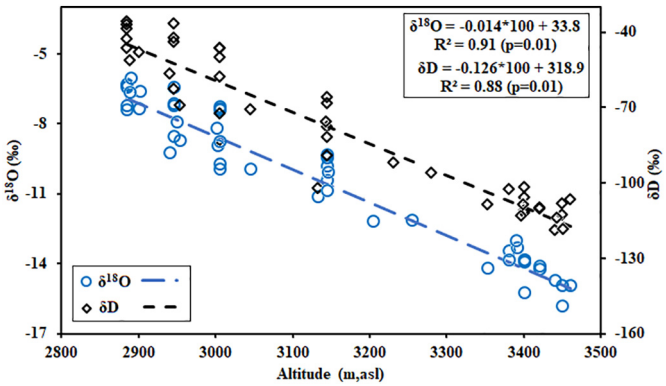

Fig. 4. Scatter plot showing the relationship of $\delta^{18}O$ and δD with altitude of precipitation in Ladakh, upper IRB.

This is attributed to the well-known altitude effect, as the altitude of Leh is higher (3450 m, amsl) than the altitude of Kargil (3144 m, amsl) and Dras (2860 m, amsl) precipitation sites. A substantial correlation (R^2 = 0.97; p = .01 and R^2 = 0.88; p = .01) exist between the mean monthly $\delta^{18}O$ (and δD) and the altitude of precipitation sites (Fig. 4). Based on 2 years of isotopic data, the estimated altitude gradient of the Ladakh, upper IRB is −0.25 to −0.58‰ and − 0.72 to −2.39‰ per 100 m rise in elevation for $\delta^{18}O$ and δD respectively. The altitudinal gradients observed are similar to those reported in other parts of the globe (Table 3). In Himalayas (Hou et al., 2001; Yao et al., 2009; Jeelani et al., 2017a, in the Alps (Poage and Chamberlain, 2001, Andes (Windhorst et al., 2013), Rocky Mountains (Moran et al., 2007), Eastern Tianshan (Pang et al., 2011), Mount Cameroon (Gonfiantini et al., 2001), Oregon, USA (McGuire et al., 2005), Taiwan (Peng et al., 2010) and Switzerland (Siegenthaler and Oeschger, 1980).

In January, the precipitation was found to be highly depleted in heavier stable water isotopes and in July, the precipitation is enriched

Table 2
Average $\delta^{18}O$, δD, D-excess and Relative Humidity in precipitation for sampling stations in Ladakh, upper Indus river basin during the sampling period.

	Drass				Kargil				Leh			
Month	$\delta^{18}O$	δD	D-excess	R.H	$\delta^{18}O$	δD	D-excess	R.H	$\delta^{18}O$	δD	D-excess	R.H
Jan	−15.4	−134	22	88	−15.8	−134	22	84	−16.1	−150	23	86
Feb	−14.9	−103	19	86	−15.1	−110	20	86	−15	−148	21	80
Mar	−13.3	−96	16	86	−13.6	−74	17	88	−14.2	−148	19	85
Apr	−12.4	−89	16	87	−11.5	−82	16	85	−13.4	−121	17	87
May	−10.1	−70	11	85	−10.5	−117	11	81	−11.7	−107	11	81
June	−8.46	−55	9	72	−8.3	−48	9	70	−10.1	−62	9	73
July	−7.30	−48	8	74	−7.4	−47	9	76	−8.9	−108	10	75
Aug	−12.2	−51	10	84	−12.8	−112	11	83	−14.8	−72	12	88
Sept	−8.31	−52	8	77	−9.8	−46	8	71	−11.6	−45	8	74
Oct	−10.9	−55	13	79	−11.45	−73	13	73	−12	−66	14	75
Nov	−11.8	−47	17	84	−12.43	−87	17	81	−12.9	−115	17	80
Dec	−13.1	−93	19	81	−13.76	−98	20	79	−14.3	−96	19	84

Table 3
Altitudinal gradients of $\delta^{18}O$ and δD in precipitation from various sites across the globe.

$\delta^{18}O$‰	δD‰	Location	Reference
−0.12 to −0.29	–	Himalayas	Hou et al., 2001
−0.31 to −0.33	–	Trans-Himalayas	Yao et al., 2009
−0.15 to −0.64	−0.85 to −2.8	Northwestern Himalayas	Jeelani et al., 2017a
−0.21 to −0.28	–	Alps	Poage and Chamberlain, 2001
−0.22	−1.12	Andes	Windhorst et al., 2013
−0.3 to +1.8	–	Rocky Mountains	Moran et al., 2007
−0.16 to −0.23	−1.0 to −1.6	Eastern Tianshan	Pang et al., 2011
−0.15 to −0.24	–	Mount Cameroon	Gonfiantini et al., 2001
−0.15	–	Oregon, USA	McGuire et al., 2005
−0.17 to −0.22	–	Taiwan, China	Peng et al., 2010
−0.09 to −0.25	–	Switzerland	Siegenthaler and Oeschger, 1980

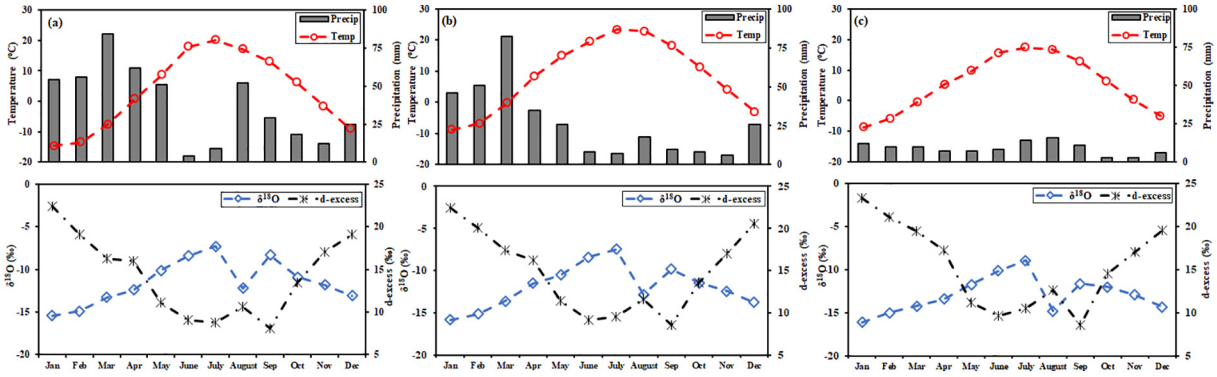

Fig. 5. Monthly variation of $\delta^{18}O$ and D-excess in precipitation at all sampling sites (a) Dras (b) Kargil (c) Leh along with average monthly precipitation and temperature across the upper Indus basin Ladakh.

in heavier stable water isotopes (Fig. 5). It is apparent in the plot (Fig. 5) that there is a progressive increase in isotopic value (i.e., enrichment of((^{18}O and ^{2}H) of precipitation from January to July and declining trend in isotopic value (i.e., depletion of ^{18}O and ^{2}H) from September to December (Fig. 5)." This is consistent with the rise in ambient temperature from the month of January to July and a decline in temperature from September to December. August is an exception, when the stable water isotopic value of precipitation abruptly drops, without much deviation in the air temperature. This appears to be due to the amount effect as the precipitation amount in August in Dras and Kargil is higher, but in Leh, there is no noteworthy rise in precipitation amount. Therefore, the precipitation amount effect does not hold good.

Looking at the d-excess of precipitation (Fig. 5) the decline in d-excess from the month of January to July with a rise in temperature indicates the temperature effect in modifying the stable water isotopic composition of rainfall. Similarly, the rise in d-excess from September to December with a reduction in temperature suggested the decreasing influence of temperature with its drop. The lower isotopic value associated with lower d-excess and high temperature in August strongly suggests the change in the source of moisture. We know that during June to September the precipitation is controlled by Indian summer monsoons across the Himalayas (Tian et al., 2003; Liu et al., 2008a, 2008b; Jeelani et al., 2017a, 2017b, 2017c). The lighter isotopic values associated with lesser d-excess in August, therefore, reflects strong incursion of Indian summer monsoons into the Ladakh region. The similar conclusions are also reported by other higher altitude regions. For example: Tibetean Plateau (Tian et al., 2001; Tian et al., 2008; Liu et al., 2008a, 2008b; Yao et al., 2013), Tianshan mountains (Yao et al., 2013; Wang et al., 2016; 2017), Kashmir valley (Jeelani et al., 2017a, 2017b; Jeelani et al., 2018). The enriched heavy stable water isotopes and lesser d-excess of rainwater in the month of July and September designate the significant influence of temperature and aridity in modifying the stable isotopic values of precipitation. This has left us with no option to link this precipitation with any airmass. The precipitation with depleted heavier stable water isotopes and high d-excess (> 15) as is reported from November to April indicates their source from western disturbances.

Looking at the d-excess of precipitation (Fig. 5) the decline in d-excess from the month of January to July with a rise in temperature indicates the temperature effect in modifying the stable water isotopic composition of rainfall. Similarly, the rise in d-excess from September to December with a reduction in temperature suggested the decreasing influence of temperature with its drop. The lower isotopic value associated with lower d-excess and high temperature in August strongly suggests the change in the source of moisture. We know that during June to September the precipitation is controlled by Indian summer monsoons across the Himalayas (Tian et al., 2003; Liu et al., 2008a, 2008b; Jeelani et al., 2017a, 2017b, 2017c). The lighter isotopic values associated with lesser d-excess in August, therefore, reflects strong incursion of Indian summer monsoons into the Ladakh region. The similar conclusions are also reported by other higher altitude regions. For example: Tibetean Plateau (Tian et al., 2001; Tian et al., 2008; Liu et al., 2008a, 2008b; Yao et al., 2013), Tianshan mountains (Yao et al., 2013; Wang et al., 2016; 2017), Kashmir valley (Jeelani et al., 2017a, 2017b; Jeelani et al., 2018). The enriched heavy stable water isotopes and lesser d-excess of rainwater in the month of July and September designate the significant influence of temperature and aridity in modifying the stable isotopic values of precipitation. This has left us with no option to link this precipitation with any airmass. The precipitation with depleted heavier stable water isotopes and high d-excess (> 15) as is reported from November to April indicates their source from western disturbances.

The gradual reduction in heavy stable water isotopes of precipitation in the course of the advancement and recession of southwest Monsoon is not a local phenomenon only restricted to the study area (Table 4). Such evolution of $\delta^{18}O$ is witnessed across the Himalayas influenced by Indian Summer Monsoons. The extent of heavy stable water isotopic depletion of precipitation in IRB is (> 10‰ in $\delta^{18}O$)

Table 4
Statistical summary of isotopic composition of precipitation in August at various stations across the Himalayas.

S.no.	Region	Altitude (m,masl)	$\delta^{18}O$‰ (Mean)	Reference
01.	Kashmir Himalayas	1500–6000	−12.4	Jeelani et al., 2017a, 2017b, 2017c
02.	Western Himalayas	1900–2600	−10.2	Kumar et al., 2010
03.	Northern Himalayas	2300–5600	−8.94	Zhao et al., 2011
04.	Eastern Himalayas	2200–5200	−14.5	Jeelani and Deshpande, 2017
05.	Central Himalayas	2700–6100	−19.5	Kang et al., 2002
06.	Middle Himalayas	1800–2400	−10.5	Liu et al., 2008a, 2008b
07.	Tibetean Plateau	3000–4533	−15	Yao et al., 2013

during Indian summer monsoons. Thermal gradients are practically non-existing during ISM; hence, they cannot be used to explain the observed gradual reduction of $\delta^{18}O$ with sea surface temperatures in the Bay of Bengal fluctuating between 28 and 29 °C (e.g. Midhun et al., 2013; Jeelani et al., 2018). During the ISM period, water availability from the external and internal environments is higher (Jeelani et al., 2018). The increased amount of vapor in the lower atmosphere during ISM makes the air column unstable and prone to convective activities. If the horizontal and vertical extent of convective systems increases as the monsoon advances, they could generate the observed gradual depletion of heavy water isotopic content in the daily precipitation during the Indian summer monsoon period.

A substantial negative relationship was found between the monthly $\delta^{18}O$ (and δD) and d-excess of the precipitation and ambient temperature as:

$$\delta^{18}O = 4.0T + 54.8\ (n = 142, R^2 = 0.73, p = 0.007) \quad (1)$$

$$D - excess = -2.39T + 40\ (n = 142, R^2 = 0.93, p = 0.001) \quad (2)$$

This suggests that temperature is one of the dominant climatological factors influencing the stable water isotopic composition of precipitation in Ladakh, upper IRB. The monthly $\delta^{18}O$ showed weak correlation ($R^2 = 0.11$) with precipitation amount (Fig. 6).

$$\delta^{18}O = -3.0P + 12.9\ (n = 142, R^2 = 0.11, p = 0.49) \quad (3)$$

This type of weak correlation is also reported in other parts of the Himalayas (Jeelani et al., 2017a, 2017b) in South Asia (Araguas-Araguas et al., 1998; Kurita et al., 2009) in Mount Cameroon (Gonfiantini et al., 2001) in Tianshan mountains (Tian et al., 2007; Pang et al., 2011; Kong et al., 2013; Wang et al., 2016) and in Beringia (Bailey et al., 2015).

6.2. Local meteoric waterline

The local meteoric waterline of Ladakh, upper IRB in India based on weighted monthly data by the least square method is.

$$\delta D = (7.4 \pm 0.2) \times \delta^{18}O + (8.3 \pm 3.9),\ (R^2 = 0.97; p < .001)$$

The slope (7.4) of LMWL is less than the GMWL and the LMWL of Tibetan Plateau (8.1) Tian et al., 2001, Kashmir Himalaya (7.9) Jeelani et al., 2017a, 2017b, 2017c, eastern Himalaya (8.1) Jeelani et al., 2017a, 2017b, 2017c central Himalayas (7.6) Kang et al., 2002, western Himalayas (7.5) Kumar et al., 2010, Eastern Tianshan (7.05) Pang et al., 2011, Okinawa Island Japan (9.3) Uemura et al., 2012a, 2012b, Hamersley Basin (6.14) Dogramaci et al., 2012 but similar to North-western China (7.4) Liu et al., 2009 and Northern China (7.4) Zhao et al., 2018 (Table 5). The lower slope of Ladakh upper (IRB) LMWL than GMWL and LMWL of other regions (Table 5) is associated with non-equilibrium conditions affecting falling rain droplets during dry conditions leading to potential for sub-cloud evaporation (Fig. 7). The drier the atmosphere, the lower the slope and intercept of the waterline will be (Liu et al., 2014; Zhao et al., 2018). The lower slopes and intercepts, reported in Northwestern china (Liu et al., 2014) and Northern China (Zhao et al., 2018) having similar climatic conditions. The difference in LMWL slope (6.9) for the month of June to September (Fig. 7b) compared to October–May (7.6) attributed to rise in air temperature during summer, which stimulates secondary evaporation (Fig. 7b). The lower intercept (7.9) for the months of June to September reflects the change in source airmass from western disturbance to the southwest monsoons. The Other Himalayan studies have reported the similar conclusions (Jeelani et al., 2017a, 2017b; Zhao et al., 2018).

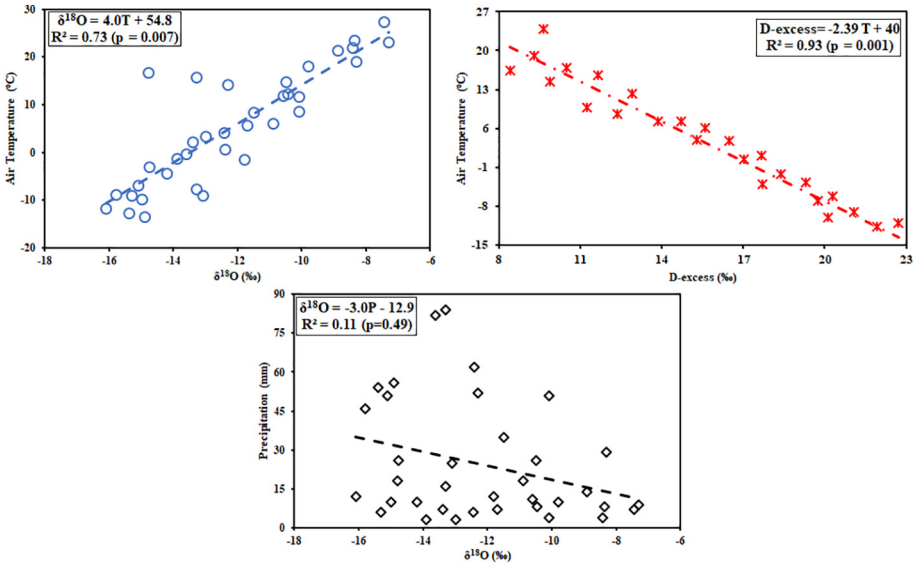

Fig. 6. The relation of $\delta^{18}O$ and D-excess with average air temperature and average precipitation amount.

Table 5
Local Meteoric Water Line of different regions across Himalayas and other parts of world.

S.no.	Region	Local meteoric water line	Reference
01.	Kashmir Himalayas	$\delta D = (7.9) \times \delta^{18}O + (16.3)$ ($R^2 = 0.97$)	Jeelani et al., 2017a, 2017b, 2017c
02.	Western Himalayas	$\delta D = (7.5) \times \delta^{18}O + (4.8)$ ($R^2 = 0.98$)	Kumar et al., 2010
03.	Eastern Himalayas	$\delta D = (8.1) \times \delta^{18}O + (12.1)$ ($R^2 = 0.98$)	Jeelani et al., 2017a, 2017b, 2017c
04.	Central Himalayas	$\delta D = (7.6) \times \delta^{18}O + (11.3)$ ($R^2 = 0.97$)	Kang et al., 2002
05.	Delingha (Tibetan Plateau)	$\delta D = (8.4) \times \delta^{18}O + (15.2)$ ($R^2 = 0.98$)	Tian et al., 2001
06.	Tianshan Mountains	$\delta D = (7.5) \times \delta^{18}O + (0.60)$ ($R^2 = 0.98$)	Pang et al., 2011
07.	Northwestern China	$\delta D = (7.4) \times \delta^{18}O + (1.38)$ ($R^2 = 0.96$)	Liu et al., 2009
08.	Okinawa Island Japan	$\delta D = (9.3) \times \delta^{18}O + (23.1)$ ($R^2 = 0.97$)	Uemura et al., 2012a, 2012b
09.	Hamersley Basin	$\delta D = (6.1) \times \delta^{18}O + (-2.7)$ ($R^2 = 0.99$)	Dogramaci et al., 2012
10.	Northern China	$\delta D = (7.5) \times \delta^{18}O + (3.2)$ ($R^2 = 0.94$)	Zhao et al., 2018

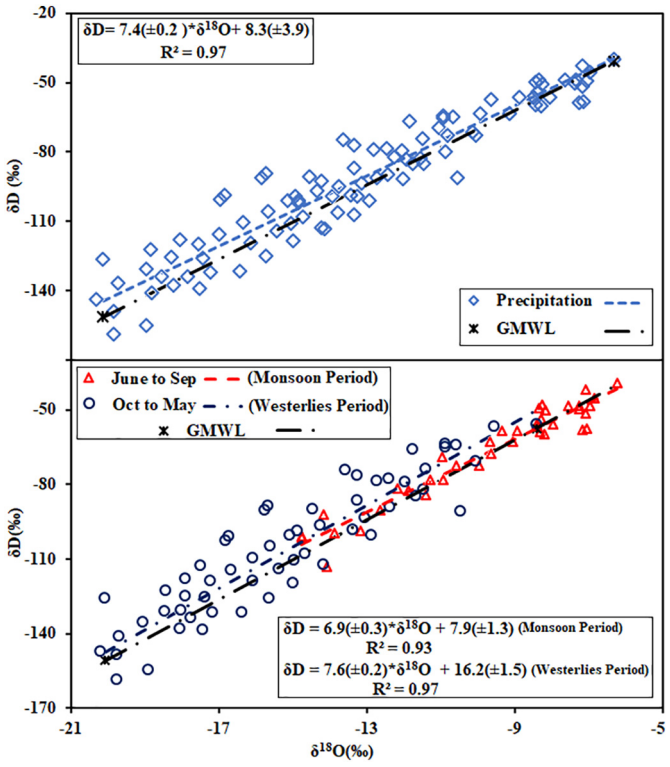

Fig. 7. The local meteroic water line of Ladakh, upper IRB based on (a) monthly data and (b) seasonal isotopic composition of the precipitation data.

7. Moisture sources analysis

The d-excess value is considered as a most vital parameter indicating regional water vapor sources (Pfahl and Sodemann, 2014; Bailey et al., 2015). The higher d-excess values in precipitation (Avg: 17‰) observed from October to April is ascribed to the moisture brought by westerlies, as the high d-excess is found in the precipitation allied with westerlies (Liu et al., 2008a, 2008b; Gat and Carmi, 1970; Jeelani et al., 2013; Yao et al., 2013; Jeelani et al., 2017a; Bershaw, 2018). The lower d-excess (Avg: 10‰) in June–September (Fig. 5) designates the vapor brought by the southwest monsoons in western Himalayas, as the lesser d-excess is found in precipitation allied with southwest monsoons (Liu et al., 2008a, 2008b; Tian et al., 2008; Breitenbach et al., 2010; Kumar et al., 2010; Yao et al., 2013; Jeelani et al., 2017a, 2017b, 2017c, Jeelani et al., 2018; Bershaw, 2018). The high relative humidity over the Arabian Sea and Bay of Bengal during summer season gives rise to lesser d-excess values in precipitation (Liu et al., 2008a, 2008b; Jeelani et al., 2017a, 2017b, 2017c). In June, July and September, the association of lower d-excess with higher $\delta^{18}O$ values, higher temperature and lower precipitation amount demonstrates the effect of evaporation on the falling rain droplets due to lower rainfall (19 mm) and reduced RH (72%) which increase evaporation and decrease d-excess of precipitation. Thus, the lesser d values perceived in August (monsoon period) are further declined in JJS. Although the definite seasonal trend in $\delta^{18}O$ is not discernible in June, July and September (JJS), there is a decline in monthly average d-excess from 17 to 10‰ in JJS (Fig. 5). The depletion of $\delta^{18}O$ in precipitation with a rise in d-excess in August indicates the humid condition, which prevents evaporation of falling raindrops. This type of isotopic signature is representative of south-west monsoons in other Himalayan regions (Tian et al., 2001; Tian et al., 2007; Tian et al., 2008; Yao et al., 2013; Jeelani et al., 2017a, 2017b; Jeelani and Deshpande, 2017; Bershaw, 2018). In order to verify the moisture source, we used the NCEP/NCAR reanalysis datasets (Fig. 8), to propose the source of the moisture entering into Ladakh, upper IRB. Using NCEP/NCAR reanalysis data datasets, the mean wind and relative humidity fields (%) at 500 hPa in 2016, were calculated over Ladakh, upper IRB and surrounding regions (Fig. 8). The results propose that the westerly wind dominantly controls the climatological conditions from the October to May and southwest monsoons dominate June to September. This corroborates above conclusions drawn from the stable water isotopic values that the change in stable isotopic values and associated d-excess is due to change of wind direction (East to west), relative humidity and therefore, moisture source. To understand the moisture source, we further used back-trajectories model to trace the air masses bringing precipitation to Ladakh (Fig. 9), using the HYSPLIT model. Fig. 7 shows the result of air-mass trajectory model analysis for 12-time intervals in 2016.

Moisture source responsible for high d-excess and depleted $\delta^{18}O$ values of precipitation, transported predominantly by the western disturbances from October to early June (Fig. 9). Conversely, moisture source contributing to precipitation with observed enriched $\delta^{18}O$ and low d-excess (June-early July) was transported by western disturbances and southwest monsoons. The trajectories of air mass that affect Ladakh, upper Indus basin from late July to late August are exclusively originating from the Bay of Bengal (Fig. 9). This is reliable with the depleted $\delta^{18}O$ and lower d-excess observed during this phase. The highly stable water isotopic value of precipitation in June and July is attributed to vaporization of rain droplets under lower relative humidity (June: 52% and July: 62%) conditions and kinetic isotopic fractionation. The lesser d-excess value of rain in August reflects the moisture derived under highly humid (79%) climatic conditions, leading to a decrease of kinetic isotope fractionation. However, the rise in d-excess in September specifies the change in moisture source, which is reliable with information for moisture sources of rainfall as examined by HYSPLIT modeling and documented airmass paths.

8. Impact of aridity on stable water isotopes

After analysing the published data available for the Kashmir Himalayas, western Himalayas, and Middle Himalayas, we find that the precipitation in IRB, Ladakh is depleted in (^{18}O and ^{2}H than the

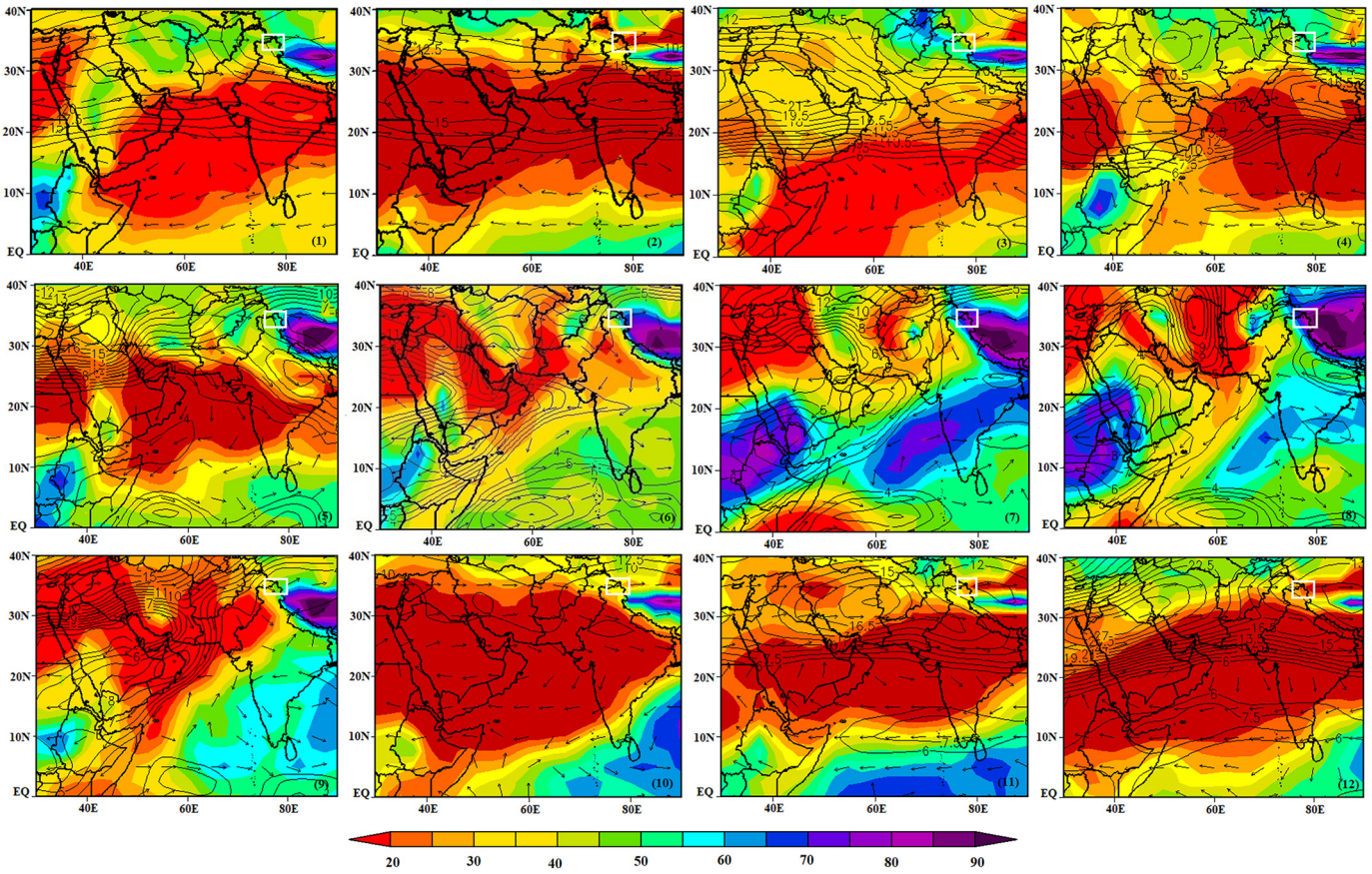

Fig. 8. The mean divergent wind vector field and specific humidity at 500 hPa pressure level in upper Indus basin during the year 2015–2016.

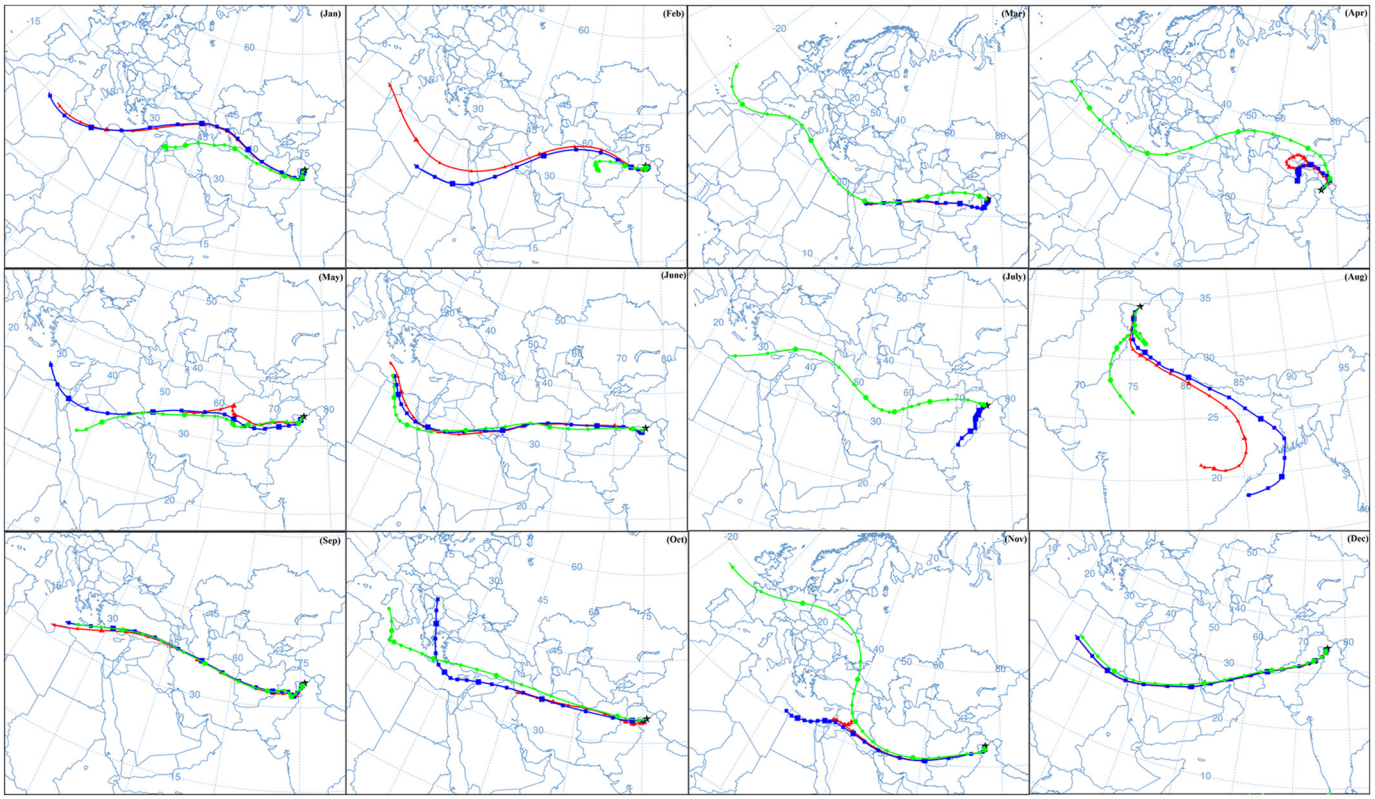

Fig. 9. HYSPLIT reverse-calculated 96-h trajectories ended at upper Indus basin. For each trajectory model, the yellow, red and blue lines in map view represent the path of air parcels terminating at (A) 1000, (B) 1500, (C) and 2000 m AGL for the 96-h period prior to the specified date for the month of 2016. (For interpretation of the references to colour in this figure legend, the reader is referred to the web version of this article.)

precipitation in Kashmir Himalayas (Jeelani et al., 2017a, 2017b, 2017c), Western Himalayas (Kumar et al., 2010) and Middle Himalayas (Liu et al., 2008a, 2008b) Table 2. This difference in stable water isotopic values of these regions is ascribed to higher altitude of Trans-Himalayas (2700–7500 m, asl) than the Kashmir Himalayas (1500–5000 m, asl), western Himalayas (1900–2600 m, asl), Middle Himalayas (3100–4500 m, asl), Eastern Himalayas [Nepal] (900-4500 m, asl) are different climatic conditions. This altitude effect should be also present in the d-excess, which is not the case. The d-excess values of the rainfall were lesser than the surrounding precipitation, which may be ascribed to the influence of arid climatic conditions prevailing in Ladakh upper IRB. The strong winds in cold arid climatic conditions of Ladakh lead to variations in atmospheric pressure allow sufficient ventilation within the porous structures of snowflakes resulting in sublimation at higher altitudes (E.g. Khardungla 6000 m, asl) and evaporation at lower elevations which in turn decreases the d-excess.

On comparing the stable water isotopic values it was apparent that the air temperature and isotopic values presented nearly similar temporal trend in the two regions (Kashmir and Ladakh region). The rainfall samples were depleted in heavier stable water isotopic values in January, which become progressively enriched in heavy water isotopic values up to July consistent with a rise in temperature. The stable water isotopic values decrease from September to December with the decline in temperature (Fig. 10). August is an exception, which is discussed above. It is essential to note here that the d-excess values of precipitation in Ladakh is unusual due to its lower value (14.8‰) than Kashmir region (17.36‰) and the monthly trend (Fig. 10). Ideally, with a reduction in temperature (or increase in altitude) the d-excess of precipitation increases with a decline in stable water isotopic value, but in Ladakh region, the d-excess of precipitation decreases. Although, d-excess shows a good correlation with ambient temperature (Fig. 6) but monthly values are very low when compared with other Himalayan studies. Another significant observation is the trend of the d-excess, which is flat to some extent during October to May in Kashmir region, progressively decreases from January to May and increases from September to December in Ladakh region. The change in monthly d-excess despite the very low ambient temperature in Ladakh suggests the significant impact of aridity in modifying the stable water isotopic values of precipitation in study area.

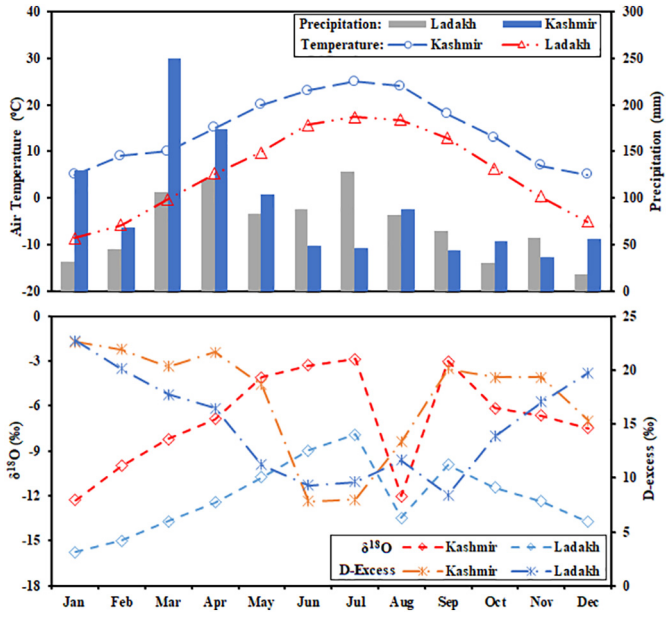

Fig. 10. Temporal variation of $\delta^{18}O$ and d-excess of precipitation in Kashmir valley and Ladakh, upper IRB.

9. Moisture source diagnostic

Lagrangian trajectory model has been widely used to distinguish the path of air masses during the particular time period (Sodemann et al., 2008; Crawford et al., 2017; Wang et al., 2017). The specific humidity variations of such an air mass determines the effect of precipitation and evaporation processes along its trajectory. Moisture variations in an air mass during a particular time interval ($\Delta q/\Delta t$) are usually the net result of vaporization (V) into precipitation (P) (Stohl and James, 2004; Sodemann et al., 2008; Wang et al., 2017).

For each 6 h interval, if the specific humidity is 0.2 g/kg higher than at the earlier time interval, and the modeled height of the air mass is below the boundary layer height, the location of air parcel at the earlier time is recognized as an evaporative source location (Sodemann et al., 2008; Wang et al., 2017). The identification of moisture uptake location is continued backward until the specific humidity reaches ≤ 0.05 g/kg, trajectory falls almost dry because of rainout (Sodemann et al., 2008; Crawford et al., 2017; Wang et al., 2017). The specific humidity data was used from National Oceanic Atmospheric Administration (NOAA).

As all deviations are calculated over a 6 h time interval, the denominator Δt is dropped for ease (Sodemann et al., 2008).

$$\frac{Dq}{Dt} \approx \frac{\Delta q}{\Delta t} = E - P\ (g\ kg^{-1}(6\ h)^{-1} \tag{4}$$

Figs.11 and 12 show sketches of air mass trajectories demonstrating how moisture is added/subtracted to a particular airmass from Mediterranean and Bay of Bengal during its travel to study area. In order to calculate the backward trajectory, the arrival point of the airmass over Ladakh is referred to as the start point ($t = 0$ h), while the initial point is called endpoint ($t = 102$ h). The dashed red line gives the progress of the airmass specific humidity (q). The Δq° bars signify moisture increase ($\Delta q^{\circ} > 0$), and below a moisture decrease ($\Delta q^{\circ} < 0$) during a 6 h time interval.

$$\Delta q^{0}(t) = q(\vec{x}\,(t)) - q(\vec{x}\,(t - 6h)) \tag{5}$$

where the superscript $^{\circ}$ indicates that the total diagnosed moisture change at a source region and $\vec{x}\,(t)$ denotes the position of an air parcel at time t. To identify the moisture source that causes the precipitation in an exact target area, only air parcel which precipitates at t = 0 are traced backward in time (Fig. 12). It is presumed that the precipitation falls whenever a relative humidity threshold of 80% is reached (Sodemann et al., 2006). The volume of precipitation at the target area is analysed from the reduction in Δq° during the last 6 h time interval and then expected to the trajectory's starting point (Sodemann et al., 2006; Sodemann et al., 2008; Wang et al., 2017). Moisture increases at the uptake locations with their unweighted contribution $\Delta q = \Delta q^{\circ}$ where Δq° is calculated from eq. (5) (1.2 g/ kg at 84 h and 0.5 g/ kg at 36 h).

10. Conclusion

In the present study, precipitation samples were collected to investigate the source, transportation, admixture of vapor sources and post-precipitation modification of stable water isotopic composition ($\delta^{18}O$ and δD) of precipitation in the high altitude Himalayan cold desert of Ladakh, upper (IRB). The average monthly $\delta^{18}O$ (and δD) of precipitation showed a negative correlation with altitude and temperature suggesting altitude and temperature are dominantly influencing the stable water isotopic composition of precipitation in Ladakh, upper IRB. In August the stable isotopic value of precipitation sharply drops, without much change in the temperature suggesting a change in moisture source substantiated by NCEP/NCAR and back trajectory analysis. Lesser d-excess values in Ladakh than other Himalayan regions suggests the impact of arid climatic conditions. The Lower slope of LMWL than GMWL and LMWL of other parts of Himalayas demonstrates the significant effect of secondary evaporation on falling rain

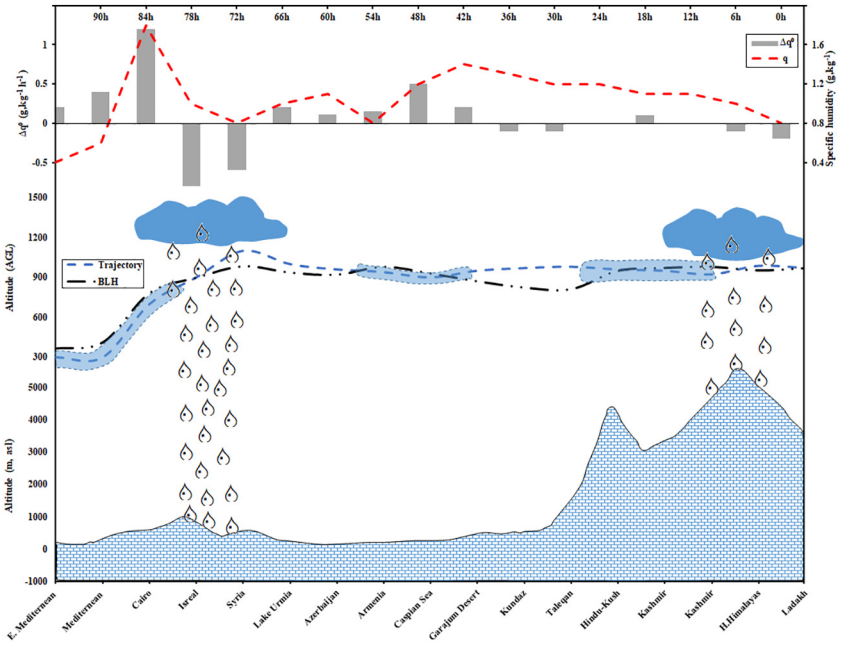

Fig. 11. Sketch of the method for identifying uptakes along a backward trajectory of an air parcel on the way from the Mediterranean Sea to Upper Indus river basin, Ladakh (blue line). Based upon the path of majority of trajectories followed. Time before arrival is given at the top. Q (red line), specific humidity in the air parcel (g/kg); Δq° change in specific humidity of an air parcel between two-time intervals (6 h) BLH, boundary layer height (black line). Thick blue sections along the trajectory denote sections of moisture increase, and over the trajectory are identified as sections of moisture decrease. (For interpretation of the references to colour in this figure legend, the reader is referred to the web version of this article.)

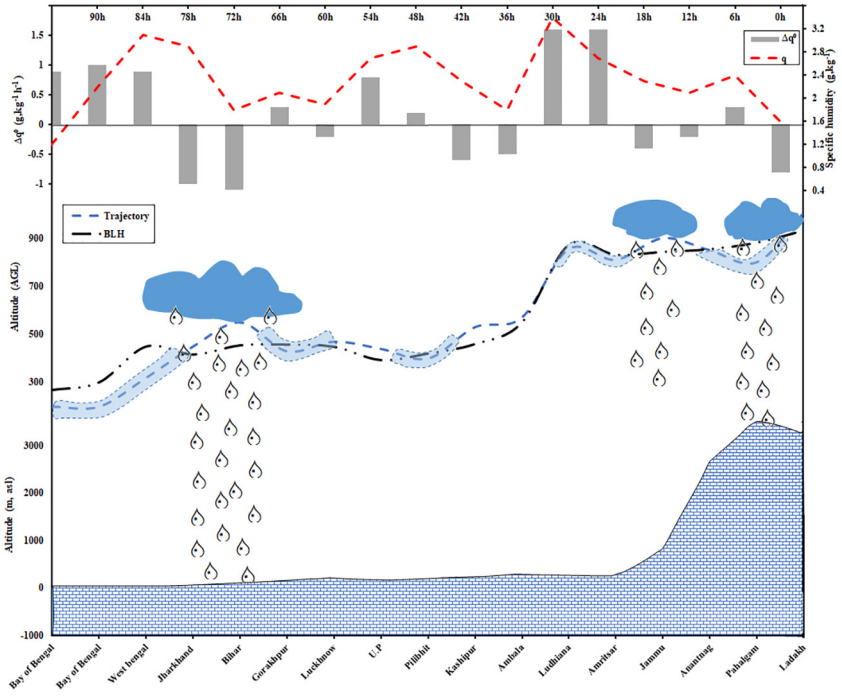

Fig. 12. Sketch of the method for identifying uptakes along a backward trajectory of an air parcel on the way from the Bay of Bengal Sea to Upper Indus river basin, Ladakh (blue line). Based upon the path of majorities of trajectories followed. Time before arrival is given at the top. Q (red line), specific humidity in the air parcel (g/kg); Δq° change in specific humidity of an air parcel between two-time intervals (6 h) BLH, boundary layer height (black line). (For interpretation of the references to colour in this figure legend, the reader is referred to the web version of this article.)

droplets below cloud base in Ladakh upper, IRB. The Lagrangian method was employed to diagnose and quantify the source of the transported path of moisture.

Acknowledgment

The work was supported by Department of science and technology (DST) GoI under Inspire Fellowship Scheme (IF: 150950) to the first author. The research work was funded by Ministry of Earth Sciences (MoES) GoI under research project (MoES/PAMC/H&C/92/2016-PC-II). The authors are thankful to editor (Jose Luis Sánchez) and anonymous reviewers for their helpful comments in improving the manuscript.

References

Breitenbach, S.F.M., Adkins, J.F., Meyer, H., Marwan, N., Kumar, K.K., Haug, G.H., 2010. The strong influence of water vapor source dynamics on stable isotopes in precipitation observed in Southern Meghalaya, NE India. Earth Planet. Sci. Lett. 292, 212–220.

Aizen, V.B., Aizen, E.M., Melack, J., et al., 1996. Isotopic measurements of precipitation on central Asian glaciers (South-eastern Tibet, northern Himalayas, central Tien Shan). J. Geophys. Res. 101 (D4), 9185–9196. https://doi.org/10.1029/96JD00061.

Aizen, V.B., Mayewski, P.A., Aizen, E.M., et al., 2009. Stable-isotope and trace element time series from Fedchenko glacier (pamirs) snow/firn cores. J. Glaciol. 55 (190), 275–291.

Araguas-Araguas, L., Froehlich, K., Rozanski, K., 1998. Stable isotope composition of precipitation over Southeast Asia. J. Geophys. Res. 103, 28721–28742.

Auer, I., Böhm, R., 1994. Combined temperature-precipitation variations in Austria during the instrumental period. Theor. Appl. Climatol. 49 (3), 161–174.

Bailey, H.L., Kaufman, D.S., Henderson, A.C.G., Leng, M.J., 2015. Synoptic scale controls on the $\delta^{18}O$ in precipitation across Beringia. Geophys. Res. Lett. 42, 4608–4616.

https://doi.org/10.1002/2015GL063983.
Bari, S.H., Rahman, M.T.U., Hoque, M.A., Hussain, M.M., 2016. Analysis of seasonal and annual rainfall trends in the northern region of Bangladesh. Atmos. Res. 176, 148–158.
Beniston, M., Rebetez, M., Giorgi, F., Marinucci, M.R., 1994. An analysis of regional climate change in Switzerland. Theor. Appl. Climatol. 49 (3), 135–159.
Bershaw, J., 2018. Controls on deuterium excess across Asia. Geosciences 8 (7), 257.
Bershaw, J., Penny, S.M., Garzione, C.N., 2012. Stable isotopes of modern water across the Himalaya and eastern Tibetan Plateau: implications for estimates of paleoelevation and paleoclimate. J. Geophys. Res. 117, D02110. https://doi.org/10.1029/2011JD016132.
Bhutiyani, M.R., Kale, V.S., Pawar, N.J., 2007. Long-term trends in maximum, minimum and mean annual air temperatures across the North-western Himalaya during the twentieth century. Clim. Chang. 85 (1–2), 159–177.
Chen, F., Zhang, M., Wang, S., Qiu, X., Du, M., 2017. Environmental controls on stable isotopes of precipitation in Lanzhou, China: an enhanced network at city scale. Sci. Total Environ. 609, 1013–1022.
Coplen, T.B., 1996. New guidelines for the reporting of stable hydrogen, carbon, and oxygen isotope ratio data. Geochim. Cosmochim. Acta 60, 3359.
Crawford, J., Hollins, S.E., Meredith, K.T., Hughes, C.E., 2017. Precipitation stable isotope variability and sub-cloud evaporation processes in a semi-arid region. Hydrol. Process. 31, 20–34. https://doi.org/10.1002/hyp.10885.
Dansgaard, W., 1964. Stable isotopes in precipitation. Tellus 16 (4), 436–468.
Diaz, H.F., Bradley, R.S., 1997. Temperature variations during the last century at high elevation sites. Clim. Chang. 36, 253–279.
Dogramaci, S., Skrzypek, G., Dodson, W., Grierson, P.F., 2012. Stable isotope and hydrochemical evolution of groundwater in the semi-arid Hamersley Basin of subtropical northwest Australia. J. Hydrol. 475, 281–293.
Draxler, R.R., Hess, G.D., 1998. An overview of the HYSPLIT_4 modeling system for trajectories, dispersion, and deposition. Aust. Meteorol. Mag. 47, 295–308.
Draxler, R., Stunder, B., Rolph, G., Stein, A., Taylor, A., 2016. HYSPLIT4 User's Guide Version 4—Last Revision: February 2016. NOAA Air Resources Laboratory, Silver Spring, Maryland.
Epstein, S., Mayeda, T., 1953. Variation of $\delta^{18}O$ content in waters from natural sources. Geochem. Cosmochim. Acta 4, 213–224.
Ferreira, R.N., Nissenbaum, M.R., Rickenbach, T.M., 2018. Climate change effects on summertime precipitation organization in the Southeast United States. Atmos. Res. 214, 348–363.
Gadgil, S., 2003. The Indian monsoon and its variability. Annu. Rev. Earth Planet. Sci. 31 (1), 429–467.
Gat, J.R., Carmi, I., 1970. Evolution of the isotopic composition of atmospheric waters in the Mediterranean Sea area. J. Geophys. Res. 75 (15), 3039–3048.
Gonfiantini, R., Roche, M.A., Olivry, J.C., Fontes, J.C., Zuppi, G.M., 2001. The altitude effect on the isotopic composition of tropical rains. Chem. Geol. 181 (1–4), 147–167.
Gröning, M., Lutz, H.O., Roller-Lutz, Z., Kralik, M., Gourcy, L., Pöltenstein, L., 2012. A simple rain collector preventing water re-evaporation dedicated for δ18O and δ2H analysis of cumulative precipitation samples. J. Hydrol. 448, 195–200.
Guan, H., Zhang, X., Skrzypek, G., Sun, Z., Xu, X., 2013. Deuterium excess variations of rainfall events in a coastal area of South Australia and its relationship with synoptic weather systems and atmospheric moisture sources. J. Geophys. Res. Atmos. 118, 1123–1138. https://doi.org/10.1002/ jgrd.50137.
Hou, S., Masson-Delmotte, V., Qin, D., Jouzel, J., 2001. Modern precipitation stable isotope vs. elevation gradients in the High Himalaya. Comment on "A new approach to stable isotope based paleoaltimetry: implications for paleoaltimetry and paleo hypsometry of the High Himalaya since the Late Miocene" by David B. Rowley et al. [Earth Planet. Sci. Lett. 188 (2001) 253–268]. Earth Planet. Sc. Lett. 209, 395–399. https://doi.org/10.1016/S0012-821X.(03)00043-8. 2003.
Jamelli, V., Pech, V.P., Chochillan, C., Brunstein, D., 2004. Geomorphic variability of debris flows and recent climate changes in the French Alps. Clim. Chang. 64, 77–102.
Jeelani, G., Deshpande, R.D., 2017. Isotope fingerprinting of precipitation associated with western disturbances and Indian summer monsoons across the Himalayas. J. Earth Syst. Sci. 126, 108.
Jeelani, G., Feddema, J.J., Veen, C.J., Stearns, L., 2012. Role of snow and glacier melt in controlling river hydrology in Liddar watershed (western Himalaya) under current and future climate. Water Resour. Res. 48 (12).
Jeelani, G., Kumar, U.S., Kumar, B., 2013. Variation of $\delta^{18}O$ and δD in precipitation and stream waters across the Kashmir Himalaya (India) to distinguish and estimate the seasonal sources of stream flow. J. Hydrol. 481, 157–165.
Jeelani, G., Shah, R.A., Fryar, A.E., Deshpande, R.D., Mukherjee, A., Jerome, P., 2017a. Hydrological processes in glacierized high altitude basins of western Himalaya. Hydrogeol. J. https://doi.org/10.1007/s10040- 017-1666-1.
Jeelani, G., Deshpande, R.D., Shah, R.A., Hassan, W., 2017b. Influence of southwest monsoons in Kashmir Valley, western Himalayas. Isot. Environ. Health Stud. 53, 400–412.
Jeelani, G., Shah, R.A., Jacob, N., Deshpande, R.D., 2017c. Estimation of snow and glacier melt contribution to Liddar stream in a mountainous catchment, western Himalaya: an isotopic approach. J. Isot. Environ. Health Stud. 53 (1), 18–35.
Jeelani, G., Deshpande, R.D., Galkowski, M., Rozanski, K., 2018. Isotopic composition of daily precipitation along the southern foothills of the Himalayas: impact of marine and continental sources of atmospheric moisture. Atmos. Chem. Phys. 18 (12), 8789–8805.
Kalnay, E., Kanamitsu, M., Kistler, R., Collins, W., Deaven, D., Gandin, L., Iredell, M., Saha, S., White, G., Woollen, J., Zhu, Y., Leetmaa, A., Reynolds, R., Chelliah, M., Ebisuzaki, W., Higgins, W., Janowiak, J., Mo, K.C., Ropelewski, C., Wang, C., Jenne, R., Joseph, D., 1996. The NCEP/NCAR 40-year reanalysis project. Bull. Am. Meteorol. Soc. 77, 437–471.
Kang, S., Kreutz, K.J., Mayewski, P.A., Qin, D., Yao, T., 2002. Stable-isotopic composition of precipitation over the northern slope of the central Himalaya. J. Glaciol. 48 (163), 519–526.
Kistler, R., Kalnay, E., Collins, W., Saha, S., White, G., Woollen, J., Chelliah, M., Ebisuzaki, W., Kanamitsu, M., Kousky, V., van den Dool, H., 2001. The NCEP–NCAR 50-year reanalysis: monthly means CD-ROM and documentation. Bull. Am. Meteorol. Soc. 82 (2), 247–268.
Kohler, T., Wehrli, A., Jurek, M., 2014. Mountains and Climate Change: A Global Concern. Sustainable Mountain Development Series. Centre for Development and Environment (CDE), Swiss Agency for Development and Cooperation (SDC) and Geographica Bernensi, Bern, Switzerland, pp. 136.
Kong, Y., Pang, Z., Froehlich, K., 2013. Quantifying recycled moisture fraction in precipitation of an arid region using deuterium excess. Tellus B 65 (1), 19251.
Kumar, U.S., Kumar, B., Rai, S.P., 2010. Stable isotope ratios in precipitation and their relationship with meteorological conditions in the Kumaon Himalayas, India. J. Hydrol. 391, 1–8.
Kurita, N., Ichiyanagi, K., Matsumoto, J., Yamanaka, M.D., Ohata, T., 2009. The relationship between the isotopic content of precipitation and the precipitation amount in tropical regions. J. Geochem. Explor. 102, 113–122.
Li, Z., Feng, Q., Wang, Q.J., Kong, Y., Cheng, A., Song, Y., Li, Y., Li, J., Guo, X., 2016. Contributions of local terrestrial evaporation and transpiration to precipitation using $\delta^{18}O$ and D-excess as a proxy in Shiyang inland river basin in China. Glob. Planet. Chang. 146, 140–151. https://doi.org/10.1016/j.gloplacha.2016.10.003.
Liu, Z.F., Tian, L.D., Yao, T.D., Yu, W.S., 2008a. Seasonal deuterium excess in Nagqu precipitation: influence of moisture transport and recycling in the middle of Tibetan Plateau. Environ. Geol. 55, 1501–1506.
Liu, Y.H., Fan, N.J., A.N, S.Q., 2008b. Characteristics of water isotopes and hydrograph separation during the wet season in the Heishui River, China, J. Hydrol. 353, 314–321.
Liu, J.R., Song, X.F., Sun, X.M., 2009. Isotopic composition of precipitation over Arid North western China and its implications for the water vapor origin. J. Geogr. Sci. 19, 164–174.
Liu, J.R., Song, X.F., Yuan, G.F., 2014. Stable isotopic compositions of precipitation in China. Tellus B 66https://doi.org/10.3402/tellusb.v66.22567. 22567.
Lone, S.A., Jeelani, G., Deshpande, R.D., 2017. Evaluating the sensitivity of glacier to climate by using stable water isotopes and remote sensing. Environ. Earth Sci. 76, 598. https://doi.org/10.1007/s12665-017-6937-6.
Lyon, S.W., Desilets, S.L., Troch, P.A., 2009. A tale of two isotopes: differences in hydrograph separation for a runoff event when using δD versus $\delta^{18}O$. Hydrol. Process. 23 (14), 2095–2101.
Maurya, A.S., Shah, M., Deshpande, R.D., Gupta, S.K., 2009. Protocol for $\delta^{18}O$ and δD analyses of water sample using Delta V plus IRMS in CF mode with gas bench II for IWIN National Programme at PRL, Ahmedabad. In: Proceedings of the 11th ISMAS Triennial Conference of Indian Society for Mass Spectrometry, Hyderabad. Indian Society for Mass Spectrometry, Mumbai, India, pp. 314–317.
McGuire, K.J., McDonnell, J.J., Weiler, M., Kendall, C., McGlynn, B.L., Welker, J.M., Seibert, J., 2005. The role of topography on catchment-scale water residence time. Water Resour. Res. 41, W05002. https://doi.org/10.1029/2004WR003657.
Midhun, M., Lekshmy, P.R., Ramesh, R., 2013. Hydrogen and oxygen isotopic compositions of water vapor over the Bay of Bengal during monsoon. Geophys. Res. Lett. 40, 6324–6328.
Moran, T.A., Marshall, S.J., Evans, E.C., Sinclair, K.E., 2007. Altitudinal gradients of stable isotopes in lee-slope precipitation in the Canadian Rocky Mountains. Arct. Antarctic Alp Res. 39 (3), 455–467.
Pang, Z., Kong, Y., Froehlich, K., Huang, T., Yuan, L., Li, Z., Wang, F., 2011. Processes affecting isotopes in precipitation of an arid region. Tellus B 63 (3), 352–359.
Peng, T.-R., Wang, C.-H., Huang, C.-C., Fei, L.-Y., Chen, C.-T.A., Hwong, J.-L., 2010. Stable isotopic characteristic of Taiwan's precipitation: a case study of western Pacific monsoon region. Earth Planet. Sci. Lett. 289, 357–366. https://doi.org/10.1016/j.epsl.2009.11.024.
Pfahl, S., Sodemann, H., 2014. What controls deuterium excess in global precipitation? Clim. Past 10, 771–781. https://doi.org/10.5194/cp-10-771-2014.
Poage, M.A., Chamberlain, C.P., 2001. Empirical relationships between elevation and the stable isotope composition of precipitation and surface waters: considerations for studies of paleo-elevation change. Am. J. Sci. 301, 1–15.
Rao, V.B., Franchito, S.H., Gerólamo, R.O.P., Giarolla, E., Ramakrishna, S.S.V.S., Rao, B.R.S., Naidu, C.V., 2016. Himalayan warming and climate change in India. Am. J. Clim. Chang. 5 (04), 558.
Rozanski, K., Araguas-Araguas, L., Gonfiantini, R., 1993. Isotopic patterns in modern global precipitation, Climate Change in Continental Isotopic Records. In: Lohmann, K.C., Swart, P.K., McKenzie, J. (Eds.), Geophysical Monograph 78. AGU, Washington, DC, pp. 136.
Salamalikis, V., Argiriou, A.A., Dotsika, E., 2015. Stable isotopic composition of atmospheric water vapor in Patras, Greece: a concentration weighted trajectory approach. Atmos. Res. 152, 93–104. https://doi.org/10.1016/j.atmosres.2014.02.021.
Sharma, K.P., Moore, B.I.I.I., Vorosmarty, C.J., 2000. Anthropogenic, climatic and hydrologic trends in the Kosi Basin, Himalaya. Clim. Chang. 47, 141–165.
Shekhar, M.S., Chand, H., Kumar, S., Srinivasan, K., Ganju, A., 2010. Climate-change studies in the western Himalaya. Ann. Glaciol. 51 (54), 105–112.
Shrestha, S., Yao, T., Adhikari, T.R., 2019. Analysis of rainfall trends of two complex mountain river basins on the southern slopes of the Central Himalayas. Atmos. Res. 215, 99–115.
Siegenthaler, U., Oeschger, H., 1980. Correlation of ^{18}O in precipitation with temperature and altitude. Nature 285, 314317.
Sodemann, H., Palmer, A., Schwierz, C., Schwikowski, M., Wernli, H., 2006. The transport history of two Saharan dust events archived in an Alpine ice core. Atmos. Chem.

Phys. 6, 667–688.
Sodemann, H., Schwierz, C., Wernli, H., 2008. Interannual variability of Greenland winter precipitation sources: lagrangian moisture diagnostic and North Atlantic Oscillation influence. J. Geophys. Res. 113 (D3).
Stohl, A., James, P., 2004. A Lagrangian analysis of the atmospheric branch of the global water cycle. Part I: method description, validation, and demonstration for the August 2002 flooding in Central Europe. J. Hydrometeorol. 5 (8), 656–678.
Tang, Y., Pang, H., Zhang, W., Li, Y., Wu, S.Y., Hou, S., 2015. Effects of changes in moisture source and the upstream rainout on stable isotopes in precipitation–a case study in Nanjing, eastern China. Hydrol. Earth Syst. Sci. 19 (10).
Tian, L., Yao, T., Numaguti, A., Sun, W., 2001. Stable isotope variations in monsoon precipitation on the Tibetan plateau. J. Meteorol. Soc. Jpn. 79, 959–966.
Tian, L., Yao, T., Schuster, P.F., White, J.W.C., Ichiyanagi, K., Pendall, E., Pu, J., Yu, W., 2003. Oxygen-18 concentrations in recent precipitation and ice cores on the Tibetan Plateau. J. Geophys. Res. 108 (D9), 4293. https://doi.org/10.1029/2002JD002173.
Tian, L., Yao, T., MacClune, K., White, J.W.C., Schilla, A., Vaughn, B., Vachon, R., Ichiyanagi, K., 2007. Stable isotopic variations in West China: a consideration of moisture sources. J. Geophys. Res. 112, D10112. https://doi.org/10.1029/2006JD007718.
Tian, L., Ma, L., Yu, W., Liu, Z., Yin, C., Zhao, Z., Tang, W., Wang, Y., 2008. Seasonal variations of stable isotope in precipitation and moisture transport at Yushu, eastern Tibetan Plateau. Sci. China Ser. D 51, 1121–1128.
Uemura, R., Masson-Delmotte, V., Jouzel, J., Landais, A., Motoyama, H., Stenni, B., 2012a. Ranges of moisture-source temperature estimated from Antarctic ice cores stable isotope records over glacial-interglacial cycles. Clim. Past 8, 1109–1125.
Uemura, R., Yonezawa, N., Yoshimura, K., Asami, R., Kadena, H., Yamada, K., Yoshida, N., 2012b. Factors controlling isotopic composition of precipitation on Okinawa Island, Japan: implications for paleoclimate reconstruction in the East Asian Monsoon region. J. Hydrol. 475, 314–322.
Villaba, R., Lara, A., Boninsegna, J.A., Masiokas, M., Delgado, S., Aravena, J.C., Roig, F.A., Schmelter, A., Wolodarsky, A., Ripalta, A., 2003. Large-scale temporal changes across the southern Andes: 20th century variations in the context of the past 400 years. Clim. Chang. 59, 177–232.
Vuille, M., Bradley, R.S., Werner, M., Keimig, F., 2003. 20th-century climate change in the tropical Andes: observations and model results. Clim. Chang. 59, 75–99.
Wang, S., Zhang, M., Hughes, C.E., Zhu, X., Dong, L., Ren, Z., Chen, F., 2016. Factors controlling stable isotope composition of precipitation in arid conditions: an observation network in the Tianshan Mountains, Central Asia. Tellus B 68, 26206. https://doi.org/10.3402/Tellus.bv68.26206.
Wang, S., Zhang, M., Crawford, J., Hughes, C.E., Du, M., Liu, X., 2017. The effect of moisture source and synoptic conditions on precipitation isotopes in arid Central Asia. J. Geophys. Res. Atmos. 122, 2667–2682. https://doi.org/10.1002/2015JD024626.
Wen, R., Tian, L.D., Weng, Y.B., et al., 2012. The altitude effect of $\delta^{18}O$ in precipitation and river water in the southern Himalayas. Chin. Sci. Bull. 57 (14), 1693–1698.
Windhorst, D., Waltz, T., Timbe, E., Frede, H.G., Breuer, L., 2013. Impact of elevation and weather patterns on the isotopic composition of precipitation in a tropical montane rainforest. Hydrol. Earth Syst. Sci. 17, 409–419.
Yang, X., Yao, T., Yang, W., Xu, B., He, Y., Qu, D., 2012. Isotopic signal of earlier summer monsoon onset in the Bay of Bengal. J. Clim. 25, 2509–2516.
Yao, T.D., Zhou, H., Yang, X.X., 2009. Indian monsoon influences altitude effect of $\delta^{18}O$ in precipitation/river water on the Tibetan plateau. Sci. Bull. 54, 2724–2731.
Yao, T., Masson-Delmotte, V., Gao, J., Yu, W., Yang, X., Risi, C., Sturm, C., Werner, M., Zhao, H., He, Y., Ren, W., 2013. A review of climatic controls on $\delta^{18}O$ in precipitation over the Tibetan Plateau: observations and simulations. Rev. Geophys. 51 (4), 525–548.
Zhao, L.J., Yin, L., Xiao, H.L., 2011. Isotopic evidence for the moisture origin and composition of surface runoff in the headwaters of the Heihe River basin. Chin. Sci. Bull. 56, 406–416.
Zhao, P., Tan, L., Zhang, P., Wang, S., Cui, B., Li, D., Xue, G., Cheng, X., 2018. Stable isotopic characteristics and influencing factors in precipitation in the monsoon marginal region of Northern China. Atmosphere 9 (3), 97.